Journal of Sound and Vibration (1999) **220**(1), 67–82
Article No. jsvi.1998.1920, available online at http://www.idealibrary.com on IDEAL

FREQUENCY DEPENDENCE OF PIPE ELBOW SHAKING FORCES GENERATED BY INTERNAL ACOUSTIC FIELDS

J. B. O'Blenes†, A. G. L. Holloway and R. J. Rogers

Department of Mechanical Engineering, University of New Brunswick, Fredericton, NB, Canada E3B 5A3

(*Received* 8 *December* 1997, *and in final form* 13 *August* 1998)

The forced vibration of a piping system due to internal acoustic waves is a frequently observed phenomenon. This paper introduces a new theoretical model for the shaking forces acting on a piping elbow. The model prediction of the restraining forces required to hold a piping elbow stationary were tested against measurements with single frequency, internal sound waves resonating within a piping system. The experiments were performed in a test rig in which the elbow is supported directly by force transducers, but isolated dynamically from the remainder of the piping. The air column contained by the pipe was driven by a loudspeaker at frequencies corresponding to its first three plane-wave modes. There was no average flow. The measurements show that both the magnitude and direction of the restraining force are affected by elbow position, measured relative to the standing wave position, and the sound frequency. The predictions from the theoretical model of the shaking force agree well with the measurements.

1. INTRODUCTION

The flow induced vibration of a piping system is a problem that can occur in circumstances where heavy gases, such as high pressure steam, are being transported through lightly supported pipes having a large pressure drop and changes in flow direction. For example, Hartlen and Jaster [1, 2] in a study of main steam–pipe vibration at the Bruce Nuclear Generating Station cite internal "organ pipe" modes driven by turbulent flow "noise" as a probable cause. There are many sources of such turbulent noise in a piping system; including valves, side-branches, elbows, and orifice plates. These noise sources are typically broadband random in nature [3] and therefore are capable of exciting modes of fluid compression having a wide range of frequencies. However, for a piping system whose diameter is small compared to its length, the plane wave modes absorb the most energy, and these can travel large distances through a piping system to produce shaking forces at remote changes in piping direction, such as elbows, or changes in pipe cross-section, such as headers. The present work was motivated by our experience

† Currently at NOVA Research and Technology Centre, Calgary, AB, Canada T2E 7K7.

0022–460X/99/060067 + 16 $30.00/0

with a piping system where the turbulent noise from a governor valve excited pressure "pulsations" having amplitudes as high as 7000 Pa (1 psi) in a 635-mm diameter pipe. Considering the pressure forces alone, this would result in peak dynamic forces of 2200 N (500 lbf). Where consecutive elbows are positioned near out-of phase pressure peaks, forces of nearly 4400 N (1000 lbf) on the intermediate piping are possible.

While there has been much work done on sound transmission through piping elbows [4], and on noise transmission through pipe walls and the response of pipe walls to internal acoustics [3, 5], there appears to be very little study of the shaking forces on a piping elbow due to internal sound waves. Existing design references (e.g., reference [6]) give only a scant treatment of pressure waves due to reciprocating pumps acting on a pipe elbow, suggesting that an estimate of the fluctuating force on a pipe elbow be calculated as the product of the maximum pressure in the piping run and the cross-sectional area of the pipe. A more complete treatment of the problem is provided by Gibert *et al*. [7] who give a formulation for a coupled pipe–fluid vibrating system. This formulation considers both a change in pipe cross-sectional area and a change in local radius of curvature (such as occurs at a pipe elbow) as a source of force. The analysis, however, does not include the rate of change of momentum of the fluid within the curved section which, as this study shows, can have a significant effect on the shaking force at higher frequencies.

The objective of the present study was to measure the forces on an elbow due to internal sound waves and compare these with a theoretical model formulated using an integral momentum balance. This study does not consider the effects of average flow through the piping system or the source of sound excitation. The experimental apparatus was built with two straight lengths of pipe and an intermediate elbow which is dynamically isolated from the piping and supported by force transducers. The air column was driven sinusoidally by a cone loud speaker at the first three resonant frequencies. Direct measurements of the shaking forces, as well as the internal pressure field, were made for various positions of the elbow relative to the standing sound waves at each frequency. The measured forces were found to compare favorably with those predicted by the theoretical model in cases where the measured pressure field matched the single frequency resonant pressure waves used in the analysis.

2. THEORETICAL MODEL

The theoretical model derived in this section provides a relationship between the restraining force required to hold the pipe elbow stationary and the amplitude and wavelength of the sound waves within it. It is based on the simplifying assumptions of a rigid pipe elbow and single frequency, resonant, plane-wave acoustic pressure and velocity fields. This analysis differs from the previous analyses of Wachel *et al*. [6] and Gibert *et al*. [7] because it includes the rate of change of fluid momentum within the elbow which is found to be significant at higher frequencies.

Figure 1 shows the control volume which is used in the analysis. It cuts through the pipe walls at each face of the elbow, perpendicular to the pipe axis, and

includes the elbow itself. The acoustic pressure and velocity within the air column are modelled as a set of plane standing waves described by the expressions

$$p(s, t) = P \sin(2\pi f t) \sin\left(\frac{2\pi f}{c} s\right), \qquad \mathbf{V}(s, t) = \frac{P}{\rho c} \cos(2\pi f t) \cos\left(\frac{2\pi f}{c} s\right) \mathbf{e}_s. \tag{1, 2}$$

Here, the $\mathbf{e}_s$ direction is taken to be locally tangent to the curvilinear co-ordinate, s, which runs along the centreline. The pressure and velocity are then constant on planes that are perpendicular to $\mathbf{e}_s$ at any position s. Thus, the wave distortion which would be required to turn the wave through the elbow is neglected, and the pressure and velocity given by equations (1) and (2) should be considered as average values over each cross-section. This approximation is good for sound frequencies that are low compared to the first acoustic cut-off frequency [4].

The force required to restrain the pipe elbow, $\mathbf{F}_R$, from the action of the acoustic waves described by equations (1) and (2) was calculated using the integral force balance [8],

$$\mathbf{F}_R + \mathbf{F}_P = \frac{\mathrm{d}}{\mathrm{d}t}\left(\iiint_{CV} \mathbf{V}\rho \, \mathrm{d}\forall\right) + \iint_{CS} \mathbf{V}\rho(\mathbf{V} \cdot \mathbf{n}) \, \mathrm{d}A, \tag{3}$$

where the weight of the elbow and fluid are neglected. $\mathbf{F}_P$ is the force resulting from the fluid pressure acting on the surface of the control volume, but, since the elbow is assumed to be surrounded by ambient pressure, it may be calculated by integrating equation (1) over the two streamwise faces. The integrals on the right hand side of equation (3) represent the rate of change of the momentum within the control volume and the net flux of momentum out of the control volume, respectively. These integrals may be evaluated from the assumed form of the velocity field described by equation (2) since the pipe elbow itself is assumed to be rigid and stationary (i.e., non-vibrating). It should be noted that $\mathbf{F}_R$ is the total

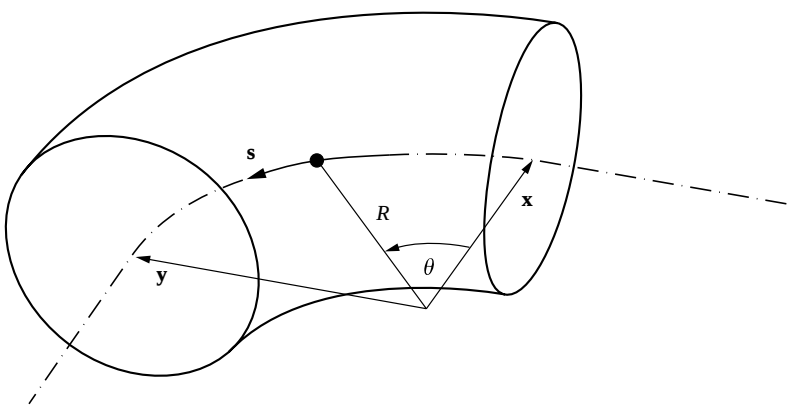

Figure 1. Control volume and co-ordinate system for an elbow.

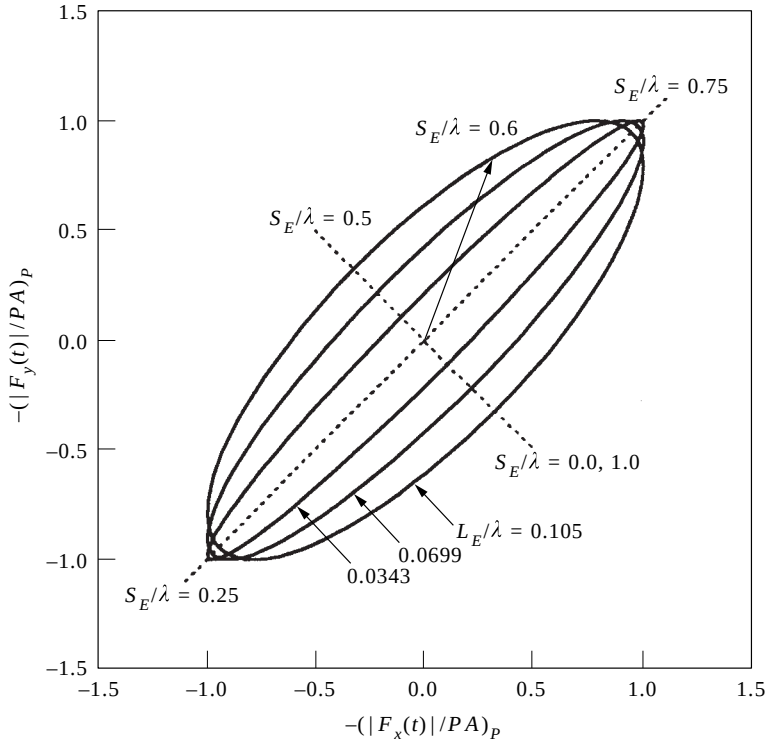

Figure 2. Ellipses formed by parametric equation (4) for the component of restraining force required to balance the pressure acting on an elbow.

restraining force and includes the pipe wall stresses and any forces provided by external supports.

It is useful at this point in the analysis to introduce a new variable S_E, which specifies the position of the elbow along the co-ordinate s, the length of the elbow L_E, and the length of the acoustic wave λ. S_E is defined as the distance from a pressure node to the mid-point along the centreline of the pipe elbow. The position of the streamwise faces of the elbow can be written as $S_E + L_E/2$ and $S_E - L_E/2$. This allows the x and y components of the pressure force $\mathbf{F}_P$ to be written as

$$\mathbf{F}_P(t) = PA \sin(2\pi ft)\left\{\begin{array}{l} \sin\left(2\pi \dfrac{S_E}{\lambda} - \pi \dfrac{L_E}{\lambda}\right) \\ \\ \sin\left(2\pi \dfrac{S_E}{\lambda} + \pi \dfrac{L_E}{\lambda}\right) \end{array}\right\}. \tag{4}$$

In the time domain, it is clear that the x and y components of the pressure force are in phase with each other. The amplitude of $\mathbf{F}_P$ depends on the ratio of elbow length to sound wavelength, and the position of the elbow relative to the sound field. Figure 2 is a plot of the amplitude of $-\mathbf{F}_P/PA$ in the (F_x, F_y) plane for the values of L_E/λ that correspond to the elbow geometry and three sound

frequencies tested in the experimental part of this study; values of S_E/λ range from 0 to 1·0 which corresponds to the elbow being moved through one full wavelength of a standing pressure wave. Because it is plotted as $-\mathbf{F}_P/PA$, this plot should be interpreted as the component of the restraining force required to balance the pressure acting on the pipe elbow.

Each ellipse in Figure 2 corresponds to a value of L_E/λ; each position on the perimeter of an ellipse corresponds to a value of S_E/λ. The maximum amplitude and direction of $\mathbf{F}_P$ is determined by drawing a line from the origin (0, 0) to the appropriate value of S_E/λ on the ellipse corresponding to the correct L_E/λ. As expected, the maximum force clearly occurs when the elbow is positioned at the pressure anti-nodes ($S_E/\lambda = 0{\cdot}25, 0{\cdot}75$). Figure 2 also shows that, as L_E/λ is increased, i.e., increasing sound frequency, the pressure force decreases slightly for an elbow positioned near a pressure anti-node ($S_E/\lambda = 0{\cdot}25, 0{\cdot}75$), whereas it increases greatly for an elbow positioned near a pressure node ($S_E/\lambda = 0{\cdot}0, 0{\cdot}5$).

The time rate of change of momentum within the control volume is found by substituting the acoustic velocity (equation (2)) into the first term on the right hand side of equation (3). Carrying out the volume integration from $S_E - L_E/2$ to $S_E + L_E/2$ and differentiating with respect to time gives the following x and y components of the shaking force due to the rate of change of momentum,

$$\mathbf{F}_V(t) = \frac{4PA\,\dfrac{L_E}{\lambda}}{16\left(\dfrac{L_E}{\lambda}\right)^2 - 1} \sin(2\pi f t)$$

$$\times \left\{ \begin{array}{l} 4\,\dfrac{L_E}{\lambda} \sin\left(2\pi\,\dfrac{S_E}{\lambda} - \pi\,\dfrac{L_E}{\lambda}\right) + \cos\left(2\pi\,\dfrac{S_E}{\lambda} + \pi\,\dfrac{L_E}{\lambda}\right) \\ \\ 4\,\dfrac{L_E}{\lambda} \sin\left(2\pi\,\dfrac{S_E}{\lambda} + \pi\,\dfrac{L_E}{\lambda}\right) - \cos\left(2\pi\,\dfrac{S_E}{\lambda} - \pi\,\dfrac{L_E}{\lambda}\right) \end{array} \right\}. \tag{5}$$

Like the pressure force, the amplitude of the rate of change of momentum forms a set of ellipses in the (F_x, F_y) plane, as shown in Figure 3. These ellipses show that, for the range of frequencies studied here, increasing the sound frequency increases the rate of change of fluid momentum linearly, i.e., a doubling of frequency produces a doubling in the major axis. At the highest frequency tested in this study, the magnitude of the rate of change of fluid momentum is 50% of the pressure force magnitude and it acts in a different direction.

It can be shown [9] that the force resulting from the net momentum flux out of the control volume (second term on right hand side of equation (3)) is very small compared to the other terms of equation (3) in the absence of an average fluid flow through the piping. The total restraining force, $\mathbf{F}_R$, calculated from equation (3) is shown in Figure 4. Note the difference between the restraining force (Figure 4) and the pressure force alone (Figure 2) which is commonly used to estimate the

restraining force. In particular, $\mathbf{F}_R$, which includes the rate of change of momentum, has a different direction than $-\mathbf{F}_P$. This is demonstrated by the force vectors for $S_E/\lambda = 0{\cdot}6$ as shown in Figures 2 and 4.

3. EXPERIMENTAL APPARATUS

Figure 5 shows the apparatus used to measure the dynamic restraint forces on the pipe elbow. The test section was open to the atmosphere and consisted of two schedule-40 ABS pipes connected with a 90° long-radius elbow. The pipe had an inside diameter of 52·5 mm (2″ nominal) and the elbow had a centreline radius of curvature of $R = 61$ mm ($L_E = 96$ mm). The lengths of the straight sections, L_1 and L_2, were varied from 80·5 to 30·5 cm in 5 cm increments. Combinations of L_1 and L_2 maintained an overall piping system length (including the elbow) of 1·206 m. See Table 1 for a summary. The coupling between the straight pipe sections and the elbow was designed to maintain a continuous acoustic path while isolating the elbow from the vibration of the straight pipes. This was done by fitting the elbow with stub pipes, and then tapering their wall thickness to produce sharp edges which were brought very close to similarly sharp edges of the straight pipes (within 0·1 mm) and covered with thin latex sleeves. The elbow itself was held in place by two uni-axial, piezoelectric force transducers (PCB model 201A) positioned so

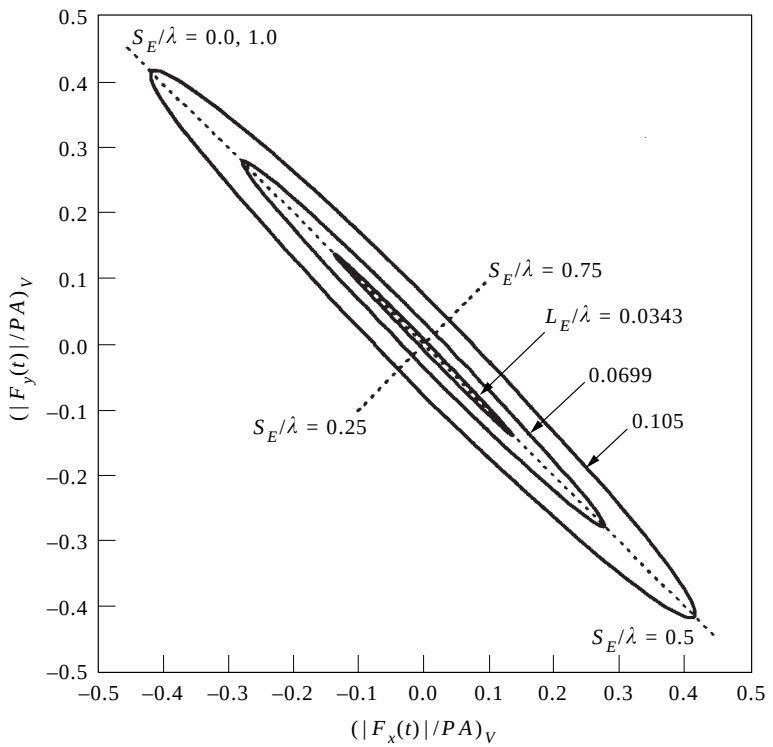

Figure 3. Ellipses formed by parametric equation (5) for the component of restraining force required to balance the momentum change within an elbow.

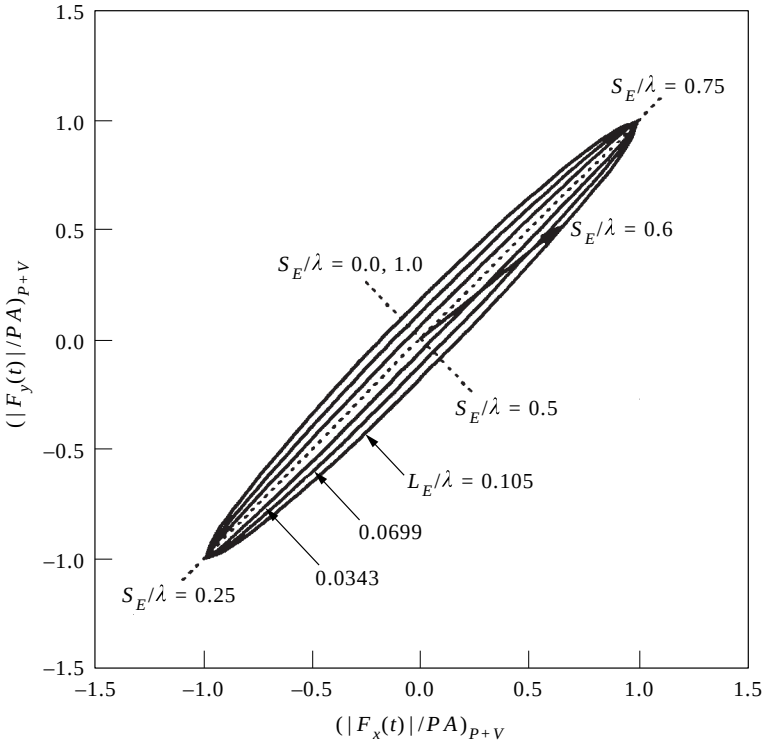

Figure 4. Total forced required to restrain a piping elbow.

their measurement axes were normal to each other and in the plane of the elbow centreline.

Calibration consisted of removing a static load normal to one transducer while the voltage from both transducers was recorded. This procedure was then repeated by removing a weight from the other transducer. The electrical signals from both

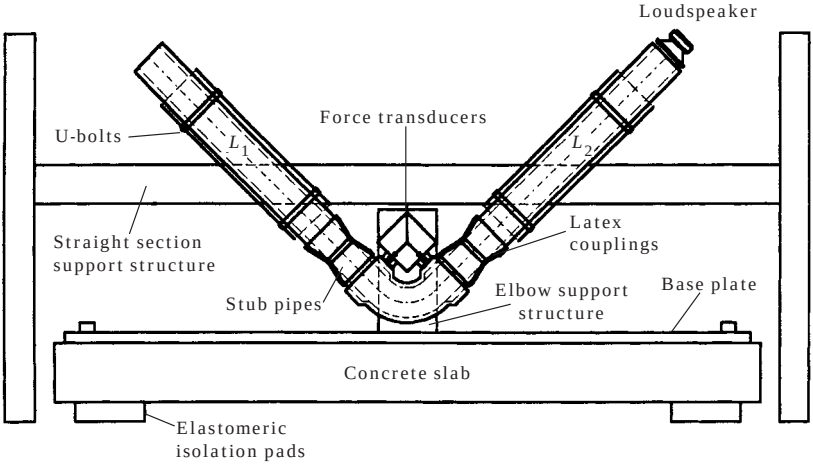

Figure 5. Experimental piping system.

TABLE 1

Pipe length combinations L_1 and L_2

L_1 (cm)	L_2 (cm)	$L_1 + L_2$ + elbow
80·5	30·5	
75·5	35·5	
70·5	40·5	
65·5	45·5	
60·5	50·5	
55·5	55·5	1·206 m
50·5	60·5	
45·5	65·5	
40·5	70·5	
35·5	75·5	
30·5	80·5	

transducers could then be combined linearly to give the components of the force. Applying a load at various angles with respect to the axes of the transducer pair showed that the error between the applied and indicated loads was always less than 7% in magnitude and less than 5° in direction. An inherent limitation of this force measurement technique, which used only two transducers, was that the calibration was strictly valid for only one value of the applied moment; this moment could not be independently determined from the transducer signals during measurement. To minimize this error, the calibration was made for zero applied moment and the transducers were positioned such that their measurement axes intersected at the centre of curvature of the elbow, a point about which the moment should be very small. The electrical signals from the force transducers were amplified, low-pass filtered, and sampled simultaneously using a 12-bit analog-digital conversion.

A cone loud speaker was placed close to, but not touching, one end of the pipe to drive the resonant sound field inside the piping system. By applying random noise, the first three resonant frequencies of this system were determined to be 123, 251 and 379 Hz. These are very close to the first three theoretical open-ended resonant frequencies and much lower than the cut-off frequency for the first non-plane mode of 3829 Hz [10]. A 12·7-mm (0·5-in.) B&K microphone fixed to the end of a long slender tube was traversed along the centreline of the open leg of the piping system (L_1) to measure the sound pressure. Typical sound pressures were 124 to 130 dB (using a reference pressure of $2{\cdot}0 \times 10^{-5}$ Pa).

4. MEASUREMENTS

Experiments were conducted for three resonance frequencies and 11 elbow positions relative to the pressure field (see Table 1 for details). For each case the sound pressure along the pipe centreline and the restraining force components were measured. In presenting these experimental results S_E was measured from the

effective end of the pipe which was determined by adding an end length correction based on the sound speed (343 m/s).

The pressure measurements are shown in Figures 6(a–c), where the curve for each elbow position is offset vertically by 0·1 units for clarity. This graph effectively shows the start of the elbow (at the end of each curve) relative to the pressure nodes; the midpoint of the elbow is $\pi R/4$ beyond the last measured point. Also shown in these figures is the "theoretical pressure field" that would be expected if the piping system behaved as an ideal one-dimensional air column with open ends.

In the case of the 123-Hz driving frequency, the pressure distribution deviated considerably from the theoretical sinusoidal wave pattern, and could be said to contain several harmonic components. This also occurred for the 251-Hz driving frequency, but to a much lesser extent. To confirm that this distortion was due to the presence of the elbow, and not due to inadequacies in the cone speaker, the elbow was replaced with a piece of straight pipe of equal centreline length. This showed a pressure distribution very close to a sinusoidal curve, and it was therefore concluded that it is not possible to establish a sinusoidal standing wave at the lower frequency with the elbow present. As a result, any comparison between the theoretical restraining force, which assumes a sinusoidal standing wave pattern, and the one measured at 123 Hz has limited validity. However, the results do serve as a demonstration of the strong effects of the elbow on the acoustic pressure field and the consequent restraining forces.

The pressure measurements for the 379-Hz driving frequency show only a slight distortion of the sinusoidal standing wave. An overview of the reaction forces measured for 379 Hz is shown in Figure 7. Each pane of the figure corresponds to a particular elbow position (shown on the graphs as S_E/λ); these can be matched up with the corresponding pressure curves in Figure 6(c). The curves correspond to the trajectory of the tip of the reaction force vector in the (F_x, F_y) plane. This figure clearly demonstrates the change in magnitude and direction of the dynamic restraining force as the elbow position is moved through the standing wave. The pane labelled "NOISE" was determined by sampling the signal from the force transducers with the loudspeaker turned off and therefore includes all electrical noise and background vibration. The total noise was 0·0017 N rms; appproximately twice the resolution of the force transducers.

The magnitude and direction of the reaction forces were determined by calculating their root mean square value and least squares fitting a line to their vector trajectories. These results are shown in Figure 8 for a 251-Hz driving frequency and Figure 9 for a 379-Hz driving frequency. The angle ϕ is measured from the bisector of the elbow for convenience. Curves showing the theoretical predictions of $\mathbf{F}_R$ and $\mathbf{F}_P$ are also shown. As noted earlier there is not only a difference in the magnitude between $\mathbf{F}_P$ and $\mathbf{F}_R$, but also a radical difference in direction. The magnitude and direction of the measured forces agree with $\mathbf{F}_R$ which includes the rate of change of momentum in its calculation. The good agreement between the theoretical estimates and the measurements of $\mathbf{F}_R$ in the case of 379 Hz is consistent with the close agreement between the assumed and measured distributions of pressure.

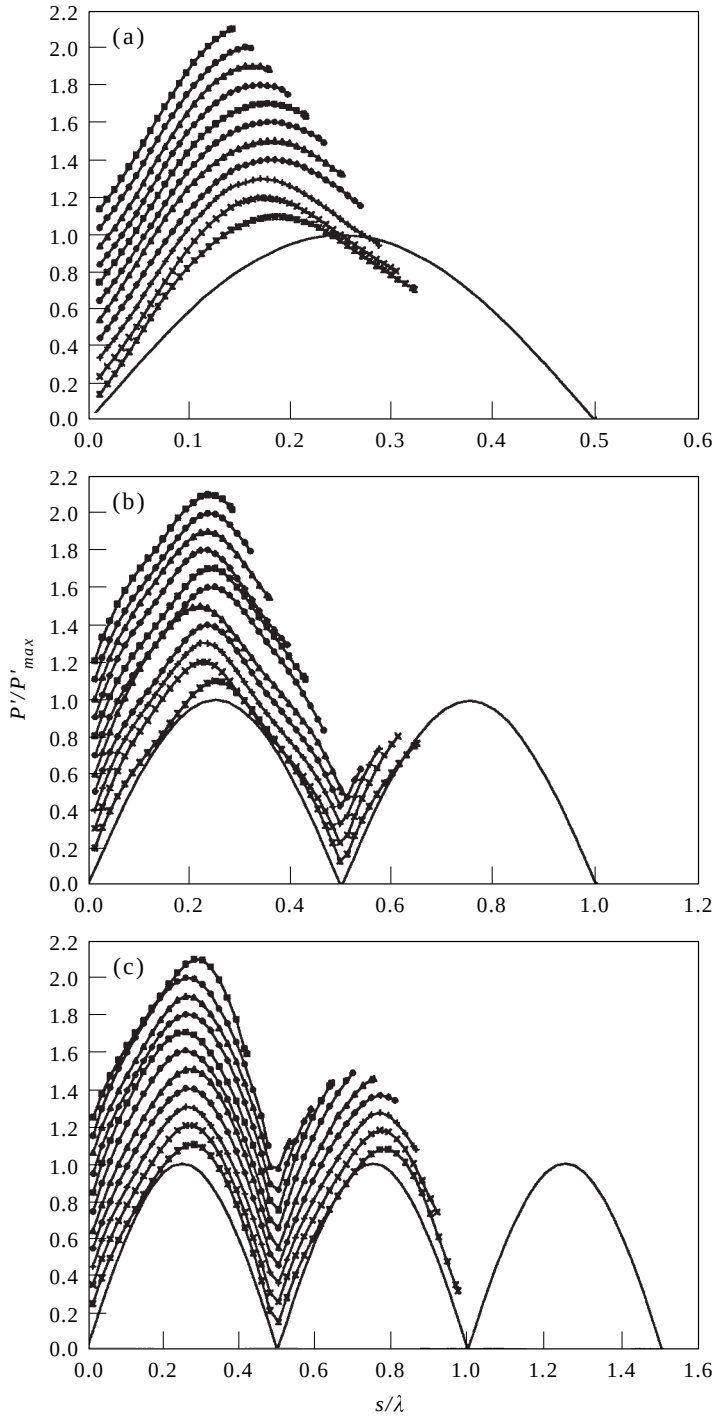

Figure 6. Measured pressure fields for first three resonant modes. (a) First mode (123 Hz) with elbow positioned at $S_E/\lambda =$ □, 0·160; ○, 0·178; △, 0·196; ◇, 0·214; ■, 0·232; ●, 0·250; ▲, 0·268; ◆, 0·286; +, 0·304; ×, 0·322; ★, 0·340; ——, theoretical pressure field. (b) Second mode (251 Hz) with elbow positioned at $S_E/\lambda =$ □, 0·317; ○, 0·354; △, 0·390; ◇, 0·427; ■, 0·463; ●, 0·500; ▲, 0·537; ◆, 0·573; +, 0·610; ×, 0·646; ★, 0·683; ——, theoretical pressure field. (c) Third mode (379 Hz) with elbow positioned at $S_E/\lambda =$ □, 0·474; ○, 0·529; △, 0·584; ◇, 0·640; ■, 0·695; ●, 0·750; ▲, 0·805; ◆, 0·860; +, 0·916; ×, 0·971; ★, 1·026; ——, theoretical pressure field.

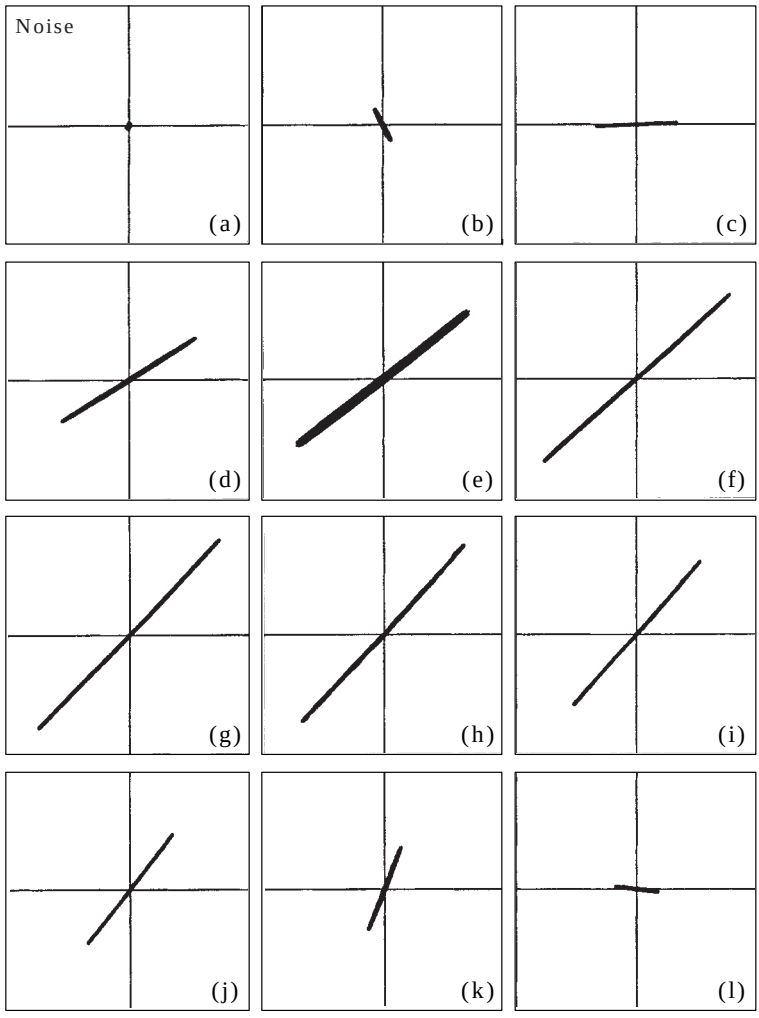

Figure 7. Trajectory of dynamic force vector on experimental elbow for various elbow positions S_E/λ. Axes limits are $-0{\cdot}25$ to $0{\cdot}25$ N for both x and y axes. $S_E/\lambda =$ (b) 0·474, (c) 0·529, (d) 0·584, (e) 0·640, (f) 0·695, (g) 0·750, (h) 0·805, (i) 0·860, (j) 0·916, (k) 0·971, (l) 1·026; (a) shows level of noise in measurement system.

To evaluate the theoretical curves shown in Figure 4 more directly, curves of this type have been constructed from the force measurements made for 379 Hz in Figure 10. The dashed lines on this graph show the vector difference between measured data points and the theoretical restraining force, $\mathbf{F}_R$.

5. DISCUSSION

The discrepancy between theory and experiment for the case of 379 Hz was less than 1% in magnitude and $1{\cdot}4^\circ$ in direction when the elbow was positioned near a pressure anti-node ($S_E/\lambda = 0{\cdot}75$) and 27% in magnitude and $43{\cdot}5^\circ$ in direction with the elbow positioned near a pressure node ($S_E/\lambda = 0{\cdot}5, 1{\cdot}0$). In the second

instance, this is substantially greater than the level of error associated with the static calibration (7% in magnitude and 5° in direction). An explanation for the large error can be based on the relatively small forces which occur when the elbow is positioned near a pressure node; the rms measurement noise level of $\mathbf{F}_N/PA = 0{\cdot}027$ is about 20% of the signal. In the 251-Hz case, the sound pressure was substantially weaker (124 versus 130 dB) and the signal to noise ratio even smaller.

The case of 123 Hz did not provide a sinusoidal sound field by which the model could be evaluated; however, it should be possible to extend the present analysis to include a multi-harmonic sound field and thereby obtain a comparison. This type of Fourier analysis could be further extended to the practical problem of having broad band excitation of all the plane wave acoustic modes.

The results from this study could be incorporated in the dynamic evaluation of a piping system design in much the same manner as existing design theory which

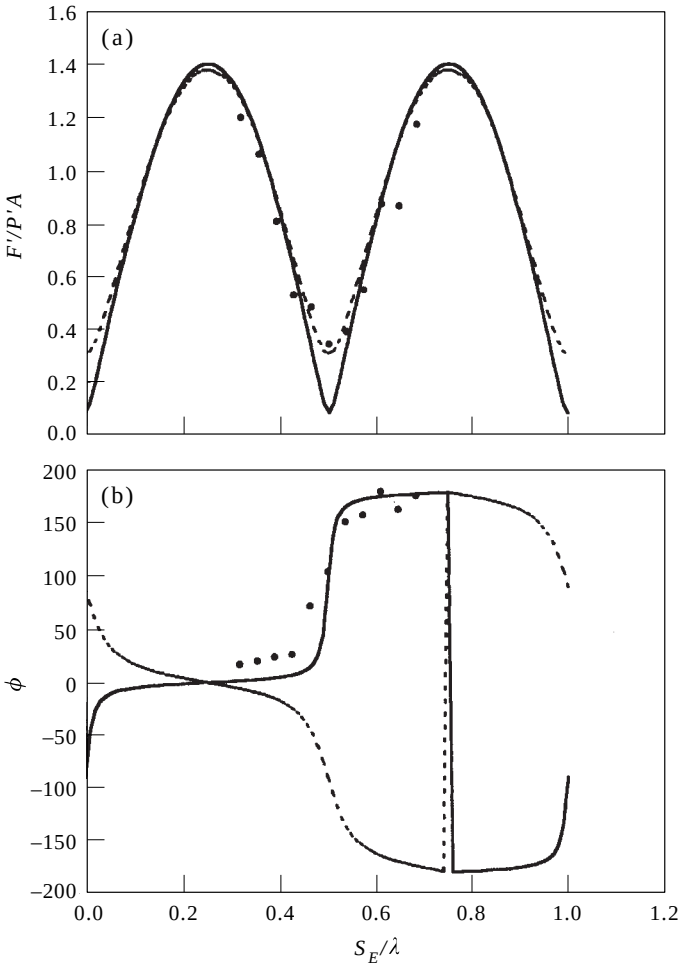

Figure 8. Normalized (a) force magnitude and (b) force direction for various elbow positions and 251 Hz driving frequency: ●, measured; - - -, $-F_P$; ——, $-F_P + F_V$.

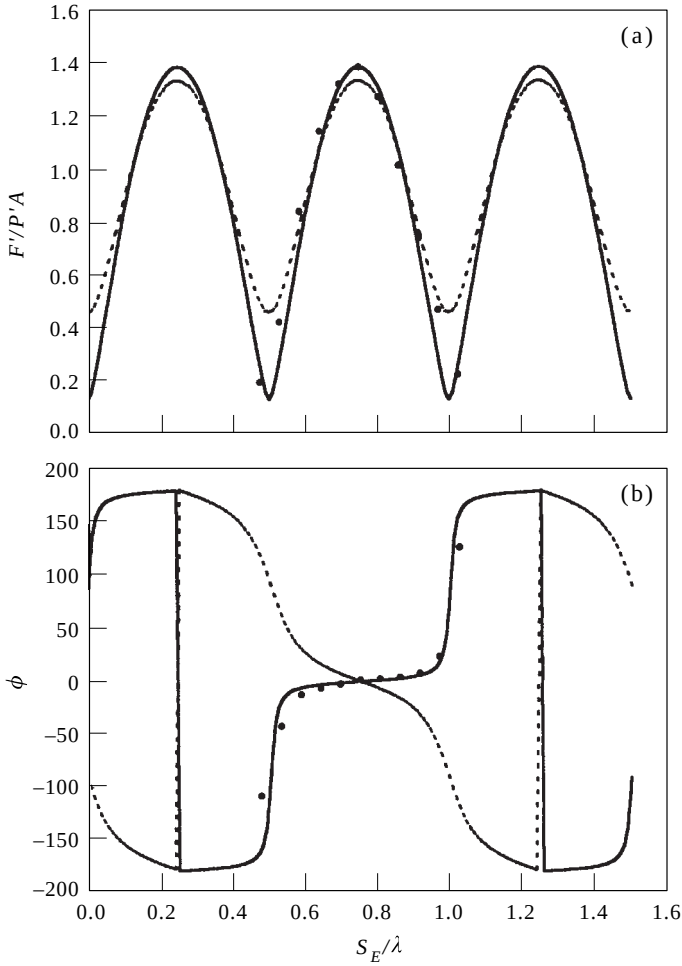

Figure 9. Normalized (a) force magnitude and (b) force direction for various elbow positions and 379 Hz driving frequency: ●, measured; - - - , $-F_P$; ——, $-F_P + F_V$.

considers only the fluid pressure. Once a model of the sound field within the piping system is generated, the total shaking force can be evaluated using the present analysis. This shaking force should be placed at the centre of curvature of the elbow. When designing pipe supports with linkage or pins (which are free to move in certain directions) the correct direction of the shaking force, as provided by this method, may be critical to achieving proper support.

The application of the present results are, in the strictest sense, limited to cases where there is no average flow through the pipe. A practical example of which is where vortex shedding excites pressure waves in a closed side branch. Most often, however, flow induced acoustics are accompanied by an average flow, and this would produce several effects not considered in this study. First, the wall turbulence and flow separation which occurs in most practical elbows would be a local source of excitation. This would combine with other sources, but the result would still be plane waves travelling along the length of the pipe. Second, the

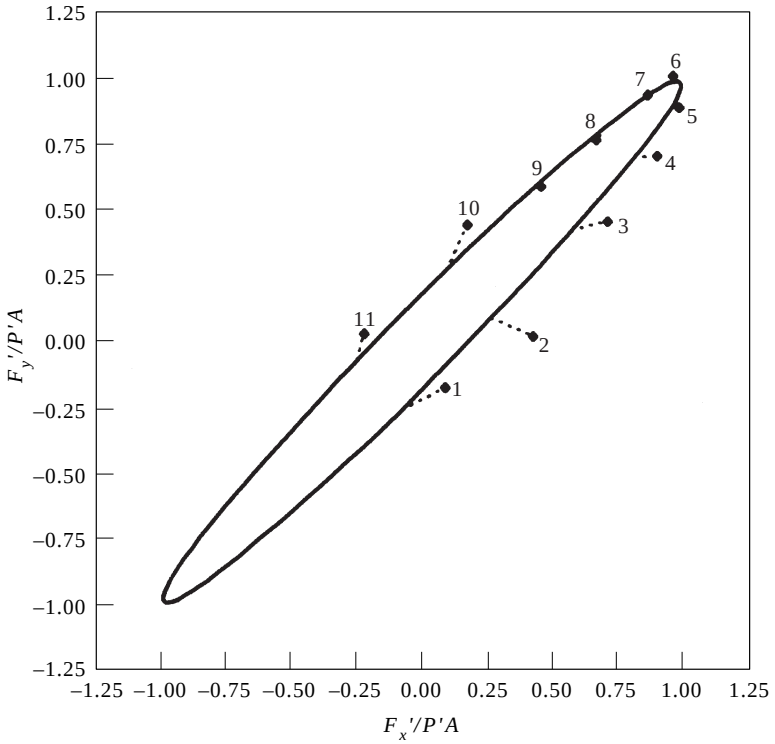

Figure 10. Measured and theoretical force on a pipe elbow for 379 Hz driving frequency: ◆, measured; ——, $-F_P + F_V$; – – –, difference.

average flow would have a Doppler effect on the frequencies and form of the resonance in the pipe. This effect would be non-uniform because of the turbulent flow distribution. In any case, this distortion scales with $(1 - \mathrm{Ma}^2)^{1/2}$, where Ma is the flow Mach number [3], and this is typically small outside of valves or similar flow restrictions in practical designs. Finally, an average flow would produce a net change of momentum having steady and fluctuating parts. The steady part would need to be supported but would not cause vibration. The fluctuating part, as determined by equation (3), would be proportional to Ma. In summary, provided that the noise sources are correctly modelled, the neglect of average flow through the elbow is a reasonable approximation where the Mach number is low.

6. CONCLUSIONS

The dynamic restraining force required to hold a pipe elbow stationary when subjected to a resonant internal sound field was measured and found to have a magnitude and direction that varies as a function of the elbow's position relative to the standing sound wave and the sound frequency. It was further demonstrated that a theoretical analysis could accurately predict the restraining force if the rate of change of momentum of the fluid within the elbow was considered. By comparison, the pressure force which acts on the elbow is only a suitable estimate

of the restraining force when the frequency is low and the elbow is located near a pressure anti-node.

ACKNOWLEDGMENTS

The authors wish to acknowledge the support of the Natural Sciences and Engineering Research Council and the University of New Brunswick for this work.

REFERENCES

1. R. T. Hartlen and W. Jaster 1978 *Ontario Hydro*, *Report No*. 78-602-*K*. Bruce NGS "A" Flow induced vibration of main steam piping: summary of research program, findings and recommendations.
2. R. T. Hartlen and W. Jaster 1979 *Practical Experiences with Flow Induced Vibrations*, *IAHR/IUTAM Symposium*, *Karlsruhe*, 144–152. Berlin: Springer. Main steam piping vibration driven by flow-acoustic excitation.
3. M. P. Norton 1989 *Fundamentals of Noise and Vibration Analysis for Engineers*. New York: Cambridge University Press.
4. A. Cummings 1974 *Journal of Sound and Vibration* **35**, 451–477. Sound transmission in curved duct bends.
5. F. J. Fahy and D. Firth 1978 *Vibration in Nuclear Plant BNES*, *Keswick*, *U.K.*, 609–615. Acoustic excitation of flexural modes in a pipe which incorporates a 90 degree radiussed bend.
6. J. C. Wachel, F. R. Szenasi, D. R. Smith, J. D. Tison, K. E. Atkins and W. R. Farnell 1985 *Vibrations in Reciprocating Machinery and Piping Systems*. Engineering Dynamics Incorporated Technical Report EDI 85-305; second edition.
7. R. J. Gibert, F. Axisa and B. Villard 1978 *Vibration in Nuclear Plant BNES*, *Keswick*, *U.K.*, 617–631. Flow induced vibration of piping system (vibration sources—mechanical response of the pipes).
8. F. M. White 1986 *Fluid Mechanics* New York: McGraw-Hill; second edition.
9. J. O'Blenes 1996 *M.Sc.E. Thesis*, *University of New Brunswick*, *Fredericton*, *NB*. Force reactions of a pipe elbow to internal gas compression waves.
10. D. D. Reynolds 1981 *Engineering Principles of Acoustics—Noise and Vibration Control*. Boston, MA: Allyn and Bacon.

APPENDIX: NOMENCLATURE

A pipe cross-sectional area
c wave speed
$\mathbf{e}_s$ unit vector tangent to piping system centreline
F force magnitude
F' rms force magnitude
$\mathbf{F}_P$ force vector due to fluid pressure
$\mathbf{F}_R$ reaction force vector
L_E elbow centreline length
p acoustic pressure
P acoustic pressure magnitude
P' rms pressure magnitude
s position along elbow centreline
S distance from pressure node
S_E elbow position relative to a pressure node

$\mathbf{V}$ fluid velocity
$\mathbf{x}$ unit direction vector
$\mathbf{y}$ unit direction vector
λ sound wavelength
ρ fluid density
ω sound frequency